Astrophys. Space Sci. Trans., 5, 39–42, 2009
www.astrophys-space-sci-trans.net/5/39/2009/

Astrophysics and Space Sciences
Transactions

Shear driven waves in the induced magnetosphere of Mars: parameter dependence

U. V. Amerstorfer[1], H. Gunell[2], N. V. Erkaev[3], and H. K. Biernat[1]

[1]Space Research Institute, Austrian Academy of Sciences, Schmiedlstr. 6, 8042 Graz, Austria
[2]Department of Physics, West Virginia University, Morgantown, WV 26506-6315, USA
[3]Institute of Computational Modelling, Russian Academy of Sciences, 660036 Krasnoyarsk-36, Russia

Received: 20 March 2009 – Revised: 2 June 2009 – Accepted: 3 July 2009 – Published: 11 September 2009

Abstract. Low frequency oscillations in the plasma in the induced magnetosphere of Mars were recently measured by the Mars Express spacecraft. Velocity shear was observed, and the plasma was shown to be Kelvin-Helmholtz unstable. In this paper we examine the effects on the frequency and growth rate of the instability when the parameters are varied around the observed values. It is found that if the velocity shear is increased by decreasing the velocity on the low velocity side, i.e. close to the planet, the growth rate increases, while a frequency consistent with the observations can be maintained. When finite Larmor radius effects are included, the growth rate depends on the direction of the vorticity and in the maximum case it is seen to increase substantially, up to a factor of 50, for narrow shear layers. This does also increase the frequency of the oscillations to a large extent.

1 Introduction

Oscillations indicative of plasma instabilities in the induced magnetospheres of the unmagnetised planets have been observed by the Pioneer Venus Orbiter (Brace et al., 1982; Russell et al., 1982) at Venus, and by Mars Global Surveyor (Espley et al., 2004), and Mars Express (Winningham et al., 2006; Gunell et al., 2008) at Mars. The induced magnetosphere is a region above the ionopause, where the magnetic field is stronger than the solar wind magnetic field. The outer boundary of the induced magnetosphere has been given several different names in the literature. We call it the Induced Magnetosphere Boundary following Lundin et al. (2004).

It has been proposed that plasma instabilities at Venus can lead to the detachment of plasmoids from the ionopause, contributing to the atmospheric escape (Brace et al., 1982). Theoretical considerations have shown that the plasma on the flanks of both Venus and Mars is unstable to the Kelvin-Helmholtz instability (Wolff et al., 1980; Penz et al., 2004; Biernat et al., 2007).

A recent comparison between observations and computational results for Mars, shows that the growth rate is too low for the Kelvin-Helmholtz instability to explain the observational data (Gunell et al., 2008). If the dayside plasma is subject to Rayleigh-Taylor interchange instability, perturbations can grow on the dayside, and these can be amplified by the Kelvin-Helmholtz instability as the plasma continues to flow down the flanks of the planet. Theoretical estimates of the growth rate of the Rayleigh-Taylor interchange instability suggest that this scenario is consistent with observations for Venus (Arshukova et al., 2004), but for Mars the growth rates are too low, except possibly in localised regions above strong crustal fields (Penz et al., 2005). A configuration similar to planetary induced magnetospheres is the heliospheric boundary layer, where at the heliopause flanks a shear layer exists between the solar wind and the interstellar plasmas. This layer could also be Kelvin-Helmholtz unstable (e.g. Baranov et al., 1992).

In this paper we use a numerical MHD model (Amerstorfer et al., 2007) to investigate how the Kelvin-Helmholtz instability is affected by varying the parameters around those used by Gunell et al. (2008) that were chosen to closely approximate the observations. In Sect. 2 we investigate the effect of increased velocity shear; in Sect. 3 we study finite Larmor radius effects.

2 Effect of velocity shear

The velocity profile used here and by Gunell et al. (2008) is given by

$$v_0(x) = \left(a_1 \tanh\left(a_2 \frac{x}{\Delta x}\right) + a_3\right) v_m \,, \quad (1)$$

Correspondence to: U. V. Amerstorfer
(ute.amerstorfer@oeaw.ac.at)

Published by Copernicus Publications on behalf of the Arbeitsgemeinschaft Extraterrestrische Forschung e.V.

Table 1. Parameters of the different cases, in all cases the magnetic field $B = 30$ nT, $k_B\, T_e = 40$ keV and $k_B\, T_i = 30$ keV.

Case	n_{O^+} (cm^{-3})	$n_{CO_2^+}$ (cm^{-3})	v_m (km s^{-1})
1	0.17	0.33	67.4
2	1	2	67.4
3	0.5	0	96.4
4	3	0	96.4

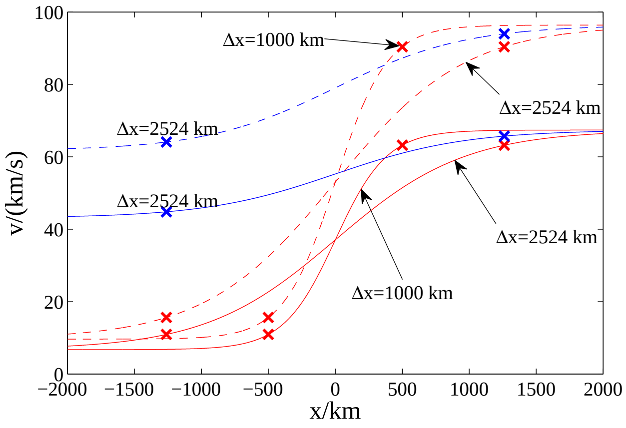

Fig. 1. Velocity profiles for the different cases. The solid lines correspond to cases 1 and 2, the dashed lines to cases 3 and 4. The blue curves show the velocity profiles that were used by Gunell et al. (2008), the red curves show the new profiles used in this work, and the crosses mark the corresponding shear layer width Δx.

where Δx is the width of the shear layer. The x-dependent equilibrium velocity $v_0(x)$ is in the y-direction. For large x, the velocity reaches its asymptotic limit v_m. As in Gunell et al. (2008), we consider cases with one ion species (O^+) and two ion species (O^+, CO_2^+). Table 1 summarizes the new cases used in this study.

Figure (1) shows the velocity profiles for different values of Δx, which are marked by crosses. The blue profiles are those which were used by Gunell et al. (2008) with $a_1 = 0.18$, $a_2 = 2.6$ and $a_3 = 0.82$. The red profiles correspond to $a_1 = 0.45$, $a_2 = 2.6$ and $a_3 = 0.55$ with a larger variation of the velocity. Although Gunell et al. (2008) did not report as large velocity variations as these and neither as small shear layer widths, similar velocity profiles are not unlikely closer to Mars.

The maximum shear is given by

$$\frac{dv_0}{dx}(x=0) = \frac{a_1 a_2 v_m}{\Delta x}.$$

The maximum frequencies and growth rates for the different maximum shears are shown in Fig. (2). The blue markers are the results by Gunell et al. (2008) with the smaller velocity variation. The growth rates for the new cases (red markers) are larger due to the larger total velocity change.

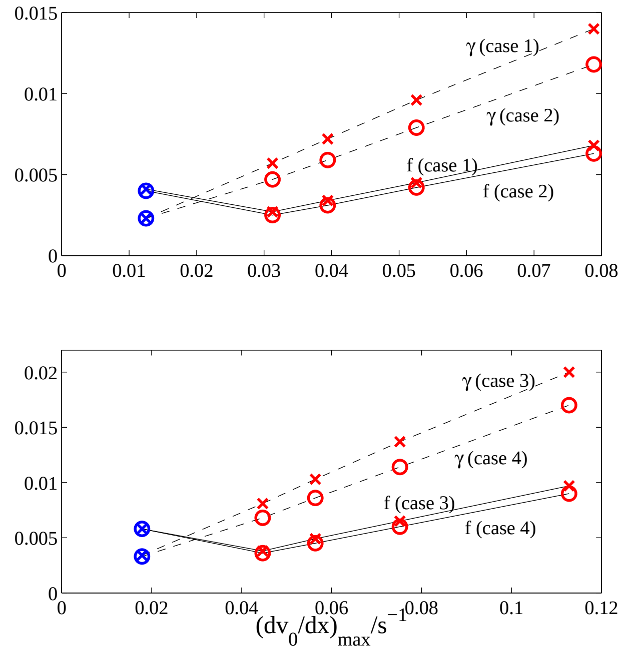

Fig. 2. Maximum frequencies (Hz, solid lines) and growth rates (s^{-1}, dashed lines) as functions of maximum shear for the cases 1 (x) and 2 (o) (top) and cases 3 (x) and 4 (o) (bottom). The values obtained by Gunell et al. (2008) are shown in blue, and new results presented here are shown in red.

Smaller Δx, i.e. larger $(dv_0/dx)_{max}$, result in larger growth rates. One interesting thing is that when the velocity variation is increased by decreasing the low-side speed (which is the case for all new cases studied in this paper), the frequency decreases while giving higher growth rates compared to the blue cases. Thus, one can get higher growth rates while still having frequencies that are consistent with the observations reported by Gunell et al. (2008).

3 Finite Larmor radius effects

So far, we have considered the theory of ideal MHD when studying the Kelvin-Helmholtz instability. However, when we decrease the width of the shear layer, such that Δx become comparable to the ion Larmor radius R_L, finite Larmor radius (FLR) effects become important and the equations of ideal MHD must be modified (e.g. Huba, 1996). The FLR MHD equations contain an additional term of the form $\nabla \cdot \mathbf{G}$ in the equation of motion, where $\mathbf{G}$ is the gyroviscosity tensor, whose components needed for this study are given by (e.g. Braginskii, 1965)

$$\mathcal{G}_{11} = -\mathcal{G}_{22} = -\rho\,\nu \left(\frac{\partial v_x}{\partial y} + \frac{\partial v_y}{\partial x}\right)$$
$$\mathcal{G}_{12} = \mathcal{G}_{21} = \rho\,\nu \left(\frac{\partial v_x}{\partial x} - \frac{\partial v_y}{\partial y}\right) \qquad (2)$$

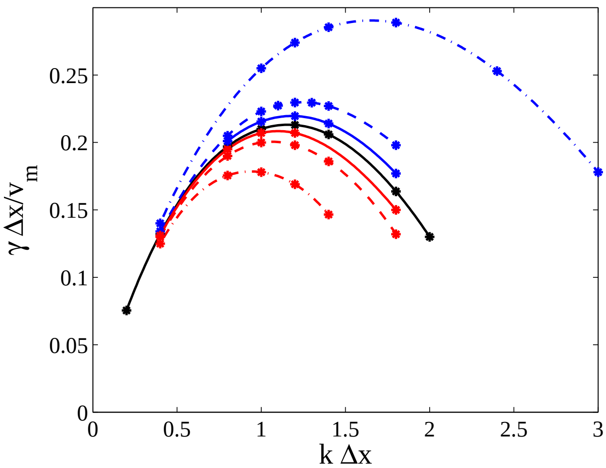

Fig. 3. Normalized growth rate as a function of the normalized wave number for different shear widths for case 3.

where ρ is the ion mass density and ν is the gyroviscous coefficient, defined as

$$\nu = \frac{k_B\,T}{2\,e\,B} \tag{3}$$

where e is the unit charge, k_B Boltzmann's constant, and T the temperature of the ions. In a multi-ion plasma, the gyroviscosity tensor is the sum of the individual gyroviscosity tensors of each ion species.

As mentioned by Huba (1996), the behaviour of the growth rate in FLR MHD depends upon the sign of $\boldsymbol{B}\cdot\boldsymbol{\Omega}$, where $\boldsymbol{B}$ is the magnetic field and $\boldsymbol{\Omega}=\nabla\times\boldsymbol{v}$ is the vorticity. As an example of the effect of the finite Larmor radius on the growth rate, Fig. (3) shows normalized growth rates as functions of the normalized wave numbers for different values of Δx for case 3. The black line corresponds to the results of ideal MHD, the blue lines to $\boldsymbol{B}\cdot\boldsymbol{\Omega}>0$ and the red lines to $\boldsymbol{B}\cdot\boldsymbol{\Omega}<0$. The solid lines give results for $\Delta x = 2524$ km, the dashed lines for $\Delta x = 1000$ km and the dashed–dotted lines for $\Delta x = 300$ km. We see that considering the finite Larmor radius either stabilizes ($\boldsymbol{B}\cdot\boldsymbol{\Omega}<0$) or destabilizes ($\boldsymbol{B}\cdot\boldsymbol{\Omega}>0$) the flow and that the effect becomes more important for smaller shear widths.

The maximum frequencies and growth rates for all four cases as a function of the ratio $R_L/\Delta x$ are shown in Figs. (4) and (5), respectively. The black lines are again the results for ideal MHD, the blue lines for $\boldsymbol{B}\cdot\boldsymbol{\Omega}>0$ and the red lines for $\boldsymbol{B}\cdot\boldsymbol{\Omega}<0$. For the cases 1 and 2 (top), the Larmor radius of CO_2^+ was taken to calculate the ratio, whereas for the cases 3 and 4 (bottom) the Larmor radius of O^+ was taken. Both the frequencies and the growth rates increase when the shear width approaches the scale of the Larmor radius, and the effect becomes more pronounced for a smaller Δx.

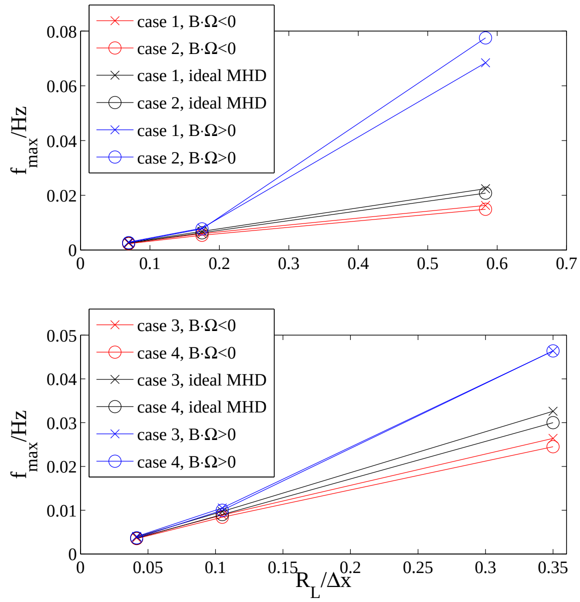

Fig. 4. Frequency of maximum growth as a function of $R_L/\Delta x$ for cases 1 (x) and 2 (o) (top) and cases 3 (x) and 4 (o) (bottom).

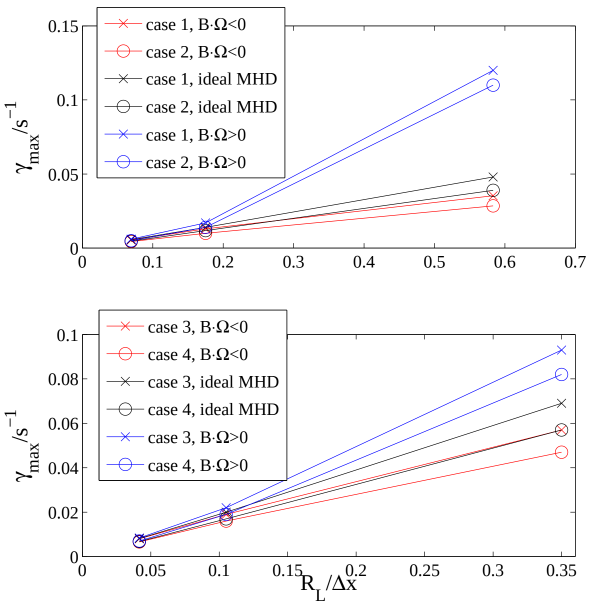

Fig. 5. Maximum growth rate as a function of $R_L/\Delta x$ for cases 1 (x) and 2 (o) (top) and cases 3 (x) and 4 (o) (bottom).

4 Conclusions

Recently reported observations and theoretical investigations of oscillations in the induced magnetosphere of Mars have shown that the Kelvin-Helmholtz instability alone might not be able to produce the observed large perturbations due to rather low growth rates (Gunell et al., 2008). However, that study motivated a closer look at the Kelvin-Helmholtz instability around Mars to investigate the behaviour of the frequencies and growth rates of the excited perturbations by varying certain parameters.

Increasing the shear by decreasing the width of the shear layer increases both the frequency and the growth rate of the instability, while increasing the shear by decreasing the velocity on the low velocity side increases the growth rate and decreases the frequency. Hence a combination of decreased minimum velocity and a narrower shear layer can lead to an increased growth rate, while the frequency remains unchanged. The observations by Gunell et al. (2008) were made downstream of the planet. Closer to the planet, the shear layer width is likely lower, and if also the velocity close to the ionosphere is lower, we would retain frequencies that are consistent with observations while the growth rates would increase by a factor of five or six, as seen in Fig. (2).

Including a finite ion Larmor radius introduces an asymmetric behaviour of the growth rate and the frequency, i.e. they are either larger or smaller compared to the ideal MHD results, depending upon the sign of $\boldsymbol{B} \cdot \boldsymbol{\Omega}$. FLR effects become important when the shear layer width is smaller than 1000 km. For $\Delta x = 300$ km the growth rate can increase a factor of about 50 (for $\boldsymbol{B} \cdot \boldsymbol{\Omega} > 0$) compared to the cases which match the observations as reported by Gunell et al. (2008). Such a large destabilizing effect has important implications when studying narrow boundary layers around planets.

Acknowledgements. This work is supported by the Austrian Science Fund (FWF) under project P21051-N16 and by the US National Science Foundation.

Edited by: H. Fichtner
Reviewed by: two anonymous referees

References

Amerstorfer, U. V., Erkaev, N. V., Langmayr, D., and Biernat, H. K.: On Kelvin Helmholtz instability due to the solar wind interaction with unmagnetized planets, Planet. Space Sci., 55, 1811–1816, doi:10.1016/j.pss.2007.01.015, 2007.

Arshukova, I. L., Erkaev, N. V., Biernat, H. K., and Vogl, D. F.: Interchange instability of the Venusian ionopause, Adv. Space Res., 33, 182–186, doi:10.1016/j.asr.2003.04.015, 2004.

Baranov, V. B., Fahr, H. J., and Ruderman, M. S.: Investigation of macroscopic instabilities at the heliopause boundary surface, Astron. Astrophys., 261, 341–347, 1992.

Biernat, H., Erkaev, N., Amerstorfer, U., Penz, T., and Lichtenegger, H.: Solar wind flow past Venus and its implications for the occurrence of the Kelvin-Helmholtz instability, Planet. Space Sci., 55, 1793–1803, doi:10.1016/j.pss.2007.01.006, 2007.

Brace, L. H., Theis, R. F., and Hoegy, W. R.: Plasma clouds above the ionopause of Venus and their implications, Planet. Space Sci., 30, 29–37, doi:10.1016/0032-0633(82)90069-1, 1982.

Braginskii, S. I.: Transport Processes in a Plasma, in: Reviews of Plasma Physics, edited by Leontovich, M. A., 1, 205–311, Consultants Bureau, New York, 1965.

Espley, J. R., Cloutier, P. A., Brain, D. A., Crider, D. H., and Acuña, M. H.: Observations of low-frequency magnetic oscillations in the Martian magnetosheath, magnetic pileup region, and tail, J. Geophys. Res., 109, A07 213, doi:10.1029/2003JA010193, 2004.

Gunell, H., Amerstorfer, U. V., Nilsson, H., Grima, C., Koepke, M., Fränz, M., Winningham, J. D., Frahm, R. A., Sauvaud, J.-A., Fedorov, A., Erkaev, N. V., Biernat, H. K., Holmström, M., Lundin, R., and Barabash, S.: Shear driven waves in the induced magnetosphere of Mars, Plasma Phys. Contr. F., 50, 074 018, doi:10.1088/0741-3335/50/7/074018, 2008.

Huba, J. D.: The Kelvin–Helmholtz instability: Finite Larmor radius magnetohydrodynamics, Geophys. Res. Lett., 23, 2907–2910, 1996.

Lundin, R., Barabash, S., Andersson, H., Holmström, M., Grigoriev, A., Yamauchi, M., Sauvaud, J.-A., Fedorov, A., Budnik, E., Thocaven, J.-J., Winningham, D., Frahm, R., Scherrer, J., Sharber, J., Asamura, K., Hayakawa, H., Coates, A., Linder, D. R., Curtis, C., Hsieh, K. C., Sandel, B. R., Grande, M., Carter, M., Reading, D. H., Koskinen, H., Kallio, E., Riihela, P., Schmidt, W., Säles, T., Kozyra, J., Krupp, N., Woch, J., Luhmann, J., McKenna-Lawler, S., Cerulli-Irelli, R., Orsini, S., Maggi, M., Mura, A., Milillo, A., Roelof, E., Williams, D., Livi, S., Brandt, P., Wurz, P., and Bochsler, P.: Solar Wind-Induced Atmospheric Erosion atMars: First Results from ASPERA-3 on Mars Express, Science, 305, 1933–1936, doi:10.1126/science.1101860, 2004.

Penz, T., Erkaev, N. V., Biernat, H. K., Lammer, H., Amerstorfer, U. V., Gunell, H., Kallio, E., Barabash, S., Orsini, S., Milillo, A., and Baumjohann, W.: Ion loss on Mars caused by the Kelvin–Helmholtz instability, Planet. Space Sci., 52, 1157–1167, doi:10.1016/j.pss.2004.06.001, 2004.

Penz, T., Arshukova, I. L., Terada, N., Shinagawa, H., Erkaev, N. V., Biernat, H. K., and Lammer, H.: A comparison of magnetohydrodynamic instabilities at the Martian ionopause, Adv. Space Res., 36, 2049–2056, doi:10.1016/j.asr.2004.11.039, 2005.

Russell, C. T., Luhmann, J. G., Elphic, R. C., Scarf, F. L., and Brace, L. H.: Magnetic field and plasma wave observations in a plasma cloud at Venus, Geophys. Res. Lett., 9, 45–48, 1982.

Winningham, J. D., Frahm, R. A., Sharber, J. R., Coates, A. J., Linder, D. R., Soobiah, Y., Kallio, E., Espley, J. R., Lundin, R., Barabash, S., Holmström, M., Andersson, H., Yamauchi, M., Grigoriev, A., Scherrer, J. R., Jeffers, S. J., Kataria, D. O., Kozyra, J. U., Luhmann, J. G., Roelof, E. C., Williams, D. J., Livi, S., Curtis, C. C., Hsieh, K. C., Sandel, B. R., Koskinen, H., Säles, T., Riihelä, P., Schmidt, W., Grande, M., Carter, M., Sauvaud, J.-A., Fedorov, A., Thocaven, J.-J., McKenna-Lawler, S., Orsini, S., Cerulli-Irelli, R., Maggi, M., Wurz, P., Bochsler, P., Krupp, N., Woch, J., Fränz, M., Asamura, K., and Dierker, C.: Electron oscillations in the induced martian magnetosphere, Icarus, 182, 360–370, doi:10.1016/j.icarus.2005.10.033, 2006.

Wolff, R. S., Goldstein, B. E., and Yeates, C. M.: The onset and development of Kelvin-Helmholtz instability at the Venus ionopause, J. Geophys. Res., 85, 7697–7707, 1980.